Declines in phytoplankton cell size in the subtropical oceans estimated from satellite remotely-sensed temperature and chlorophyll, 1998–2007

Jeffrey J. Polovina *, Phoebe A. Woodworth

NOAA, Pacific Islands Fisheries Science Center, 2570 Dole St., Honolulu, HI, USA

ARTICLE INFO

ABSTRACT

Satellite remotely-sensed sea surface temperature (SST) and surface chlorophyll were used to estimate median phytoplankton cell size at monthly and 11 km^2 resolution over the global ocean, 1998–2007. The temporal dynamics of median phytoplankton cell size were examined for the Pacific equatorial upwelling region and the subtropical oceans. For the equatorial upwelling region, cell size varied coherently with the El Niño Southern Oscillation with smaller (larger) median cell size during El Niños (La Niñas). Specifically, estimated median cell diameter increased by 34% between the 1998 El Nino and the 1999–2001 La Nina. In the subtropical oceans, over the period 1998–2007, median cell diameter exhibited statistically significant linear declines of about 2% in the North and South Pacific, and 4% in the North Atlantic. Pooling the data over all subtropical oceans, over the period 1998–2007, global median cell diameter declined by about 2%.

These results suggest that phytoplankton cell size may vary on interannual and decadal scales resulting in changes in food chain length and hence energy transfer to higher trophic levels. Further, a shift to smaller sized phytoplankton has been hypothesized as a response to ocean warming. Thus, this approach, estimating phytoplankton cell size from remotely-sensed temperature and chlorophyll, has the potential to provide global monitoring of an aspect of phytoplankton community structure likely to be responsive to future climate change.

Published by Elsevier Ltd.

1. Introduction

The energy flow from the base of the food web to higher trophic levels depends on both the amount of primary production and phytoplankton size structure. Size structure is important because energy flow in marine pelagic food webs is largely based on size specific predator–prey relationships. Thus a shift to smaller (larger) sizes at the base of the food web can increase (decrease) the number of trophic levels in the food web to any predator of a given size, which if primary production remains unchanged reduces (increases) the total energy transferred to that predator (Sprules and Munawar, 1986).

Satellite remotely-sensed ocean color provides a unique and extremely valuable global perspective on the temporal and spatial dynamics of the aspects of the marine phytoplankton community including surface chlorophyll density, primary production, and phytoplankton community composition (Yoder et al., 2010). In particular, a variety of analytical approaches have been developed and applied to estimate phytoplankton community composition from satellite remotely-sensed ocean color data (Alvain et al.,

2005; Brewin et al., 2011; Kostadinov et al., 2010; Hirata et al., 2011; Uitz et al., 2010). These approaches generally estimate relative or absolute abundance of phytoplankton by phytoplankton functional types (PFT) for 3 PFTs—picoplankton ($< 2\ \mu m$), nanoplankton (2–$20\ \mu m$) and microplankton ($> 20\ \mu m$). However, recently an alternate approach to estimate aspects of phytoplankton size structure, including median phytoplankton size, has been developed using both satellite remotely-sensed sea surface temperature (SST) and chlorophyll (Barnes et al., 2011). While SST and chlorophyll are often highly correlated it appears that the inclusion of SST with chlorophyll in the prediction model is useful as observations and ecological theory predict that variation in temperature alone can alter phytoplankton size (Moran et al., 2010; Daufresne et al., 2009). Further mesoscosm studies have shown that both temperature and nutrients work together in determining the contribution of picoplankton to the community (Agawin et al., 2000). An estimate of median phytoplankton size not only provides information on the phytoplankton size structure but it also can potentially be used with size-based models (Blanchard et al., 2009) to estimate a full ecosystem size–structure.

The use of satellite remotely-sensed data to monitor spatial and temporal dynamics of phytoplankton size has considerable appeal in understanding pelagic ecosystem dynamics and in

---

particular ecosystem impacts from climate change. In this paper we use the Barnes et al. (2011) equation to estimate the median phytoplankton size on a monthly and 11 km^2 resolution in the global ocean over the past decade with Sea-viewing Wide Field-of-view Sensor (SeaWiFS) ocean color and Pathfinder SST data. We then use these data to examine the temporal dynamics of phytoplankton median size in the equatorial upwelling region and in the subtropical oceans over the period 1998–2007.

2. Data and methods

A model predicting the median phytoplankton cell weight (M_{B50}) within a water sample at any specific location as a function of satellite remotely-sensed SST and chlorophyll-a (Chl) was derived from 361 water samples collected from 12 ocean regions that include tropical, oligotrophic, upwelling, and temperate ecosystems (Barnes et al., 2011). The equation is

$$\log_{10}(M_{B50}) = 1.340 - 0.043(SST) + 0.929(\log_{10}(Chl)) \qquad (1)$$

The predictive equation has an F-statistic of 178.6 with 2 and 358 degrees of freedom ($p < 0.001$) with an adjusted R^2 of 0.50 (Barnes et al., 2011 Suppl. mater. Table 2, http://plankt.oxfordjournals.org). While the Barnes et al. (2011) paper provides predictive equations for several size structure parameters, we chose to focus solely on the median phytoplankton cell weight (M_{B50}) as it appears to be the most intuitive. Further the statistics associated with the M_{B50} predictive equation documented that it was the variable with the highest predictive variance explained (Barnes et al., 2011 Suppl. mater., http://plankt.oxfordjournals.org).

Phytoplankton cell size is frequently expressed as cell diameter or categories based on cell diameter (picoplankton, nanoplankton, microplankton) which we find easier to interpret than weight. We convert M_{B50} to the equivalent spherical diameter (in units of μm) which we denote as M_{D50} with the relationship reported for taxonomically diverse protist plankton (Menden-Deuer and Lessard, 2000):

$$\text{cell mass} = 0.216(\text{cell volume})^{0.939} \qquad (2)$$

which results in the equation:

$$M_{D50} = 2.14(M_{B50})^{0.35} \qquad (3)$$

For all subsequent analysis we will use M_{D50} which represents the cell diameter corresponding to the median cell weight.

The satellite remotely-sensed chlorophyll-a used in the model derivation was SeaWiFS. The SeaWiFS chlorophyll-a time series began in late 1997 and ran continuously through 2007 but from 2008 forward, due to issues with the sensor, there have been months when no data was collected, so we use only data from the period 1998–2007.

The Barnes et al. (2011) equation used Moderate-resolution Imaging Spectroradiometer (MODIS) SST but that was only available beginning in December 2002. Thus to obtain monthly SST over the period 1998 through 2007, we use the 4 km Pathfinder Version 5 SST Project (Pathfinder V5) representing the latest reanalysis of the Advanced Very High Resolution Radiometer (AVHRR) data stream developed by the University of Miami's Rosenstiel School of Marine and Atmospheric Science (RSMAS) and the NOAA National Oceanographic Data Center (NODC). The SST 4 km^2 data is re-gridded to match the SeaWiFS data 11 km^2 resolution and gridding.

We estimated and compared monthly median phytoplankton size using MODIS and Pathfinder SSTs over the period of overlap (2003–2007) for the North Pacific subtropical region. The correlation between the two estimates was 0.9978 and the difference in median phytoplankton diameter less than 0.01 μm for any month.

Thus we feel comfortable substituting Pathfinder SST for MODIS SST in Eq. (1).

Persistent cloud cover results in missing data for both satellite remotely sensed SST and chlorophyll. For most months in the North Pacific, the estimated M_{D50} data time series in the subtropics (below 30°N latitude) has good coverage (less than 10% and often less than 5% of the total monthly observations missing due to cloud cover). However, in several summer months, particularly July, August, and September, due to some upwelling in the eastern Pacific and the northward movement and intensification of the Inter-tropical Convergence Zone (ITCZ), the missing data can reach as much as 20% of the total data. Above 30°N latitude, missing data generally exceeds 20% per month and reaches up to 60% of the total data in winter months due to large storms and seasonal ice cover and darkness. As a result of the substantial data loss in high latitudes we restrict our analysis of phytoplankton cell size dynamics to data from the subtropics. Specifically we considered the northern and southern hemisphere subtropical oceans defined as the area between 10 and 30°N latitude and 10 and 30°S latitude, respectively. We also consider the phytoplankton cell size dynamics time series from the Pacific equatorial upwelling region with its dynamic El Niño Southern Oscillation (ENSO) forcing, defined as 10°N–10°S latitude, east of 180° longitude.

In our analysis of the temporal dynamics of the median cell size, we use a generalized additive model (GAM) in the R programming language to fit a monthly smoother and linear time trend to the M_{D50} monthly time series averaged over the subtropical band for each ocean.

3. Results

Based on Eqs. (1) and (3), we generated a monthly phytoplankton cell size (M_{D50}) data set from 1998–2007 over the global ocean. For example, maps of North Pacific phytoplankton cell diameter distributions for February and August 2002 show median cell diameters of less than 1 μm in the most oligotrophic western subtropical North Pacific, 1–2 μm in the rest of the subtropical and equatorial waters, and diameters from 3 μm and larger in the subarctic, with the largest sizes found in northern coastal waters (Fig. 1).

The Pacific equatorial upwelling region is well-known for its strong ENSO-forced temporal phytoplankton dynamics so we examined the temporal dynamics of M_{D50} in this region. The median phytoplankton cell size averaged over the eastern equatorial Pacific shows variation coherent with ENSO events, median cell diameter decreases during El Niños and increases during La Niñas (Fig. 2). For example from the 1998 El Niño to the peak of the 1999–2001 La Niña M_{D50} increased about 34% from 1.1 to 1.5 μm (Fig. 2).

Next we examined the results from the fit of the GAM to M_{D50} for the subtropical oceans. The GAM fit all five oceans well with all adjusted R^2 exceeding 0.92. The median cell size exhibited seasonal variation in all oceans with the largest median cell size in the first quarter and the smallest in the third quarter for the northern hemisphere and the opposite pattern for southern hemisphere oceans. With the seasonal component removed from the monthly data, a liner trend was fit to the M_{D50} in each ocean. Three subtropical oceans, North Pacific, South Pacific, and North Atlantic, had statistically significant ($p < 0.05$) declining linear trends (Table 1, Fig. 3). The South Atlantic and South Indian Oceans exhibited trends that were not statistically significant. The North Pacific and South Pacific subtropical oceans had initial M_{D50} diameters of 1.05 and 1.09 μm respectively which declined by 2.2% and 2.3% respectively, over the period 1998–2007 (Table 1,
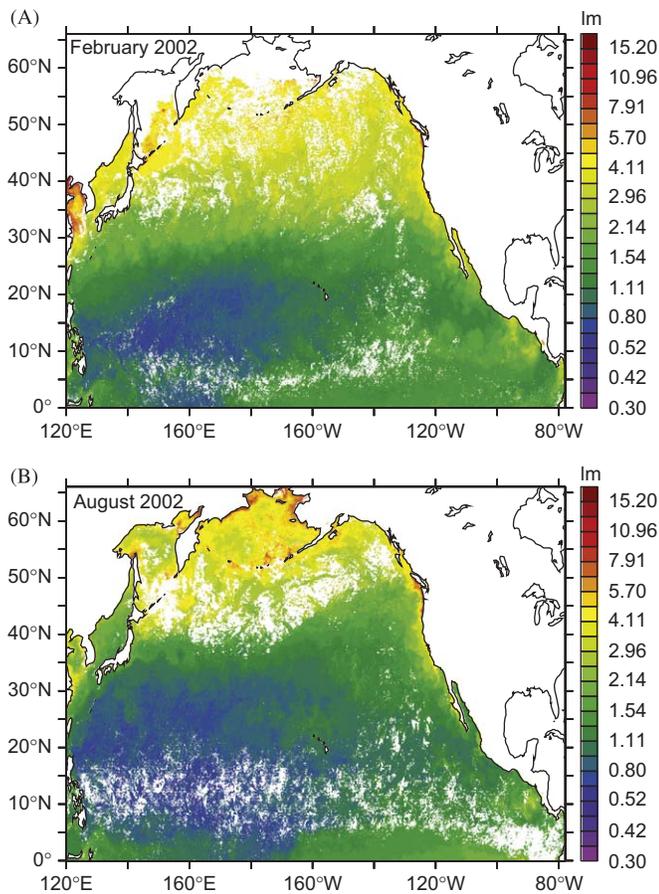
(A)

(B)

Fig. 1. Distribution of phytoplankton median cell diameter estimated using remotely sensed variables over the North Pacific for February (A) and August (B), 2002.
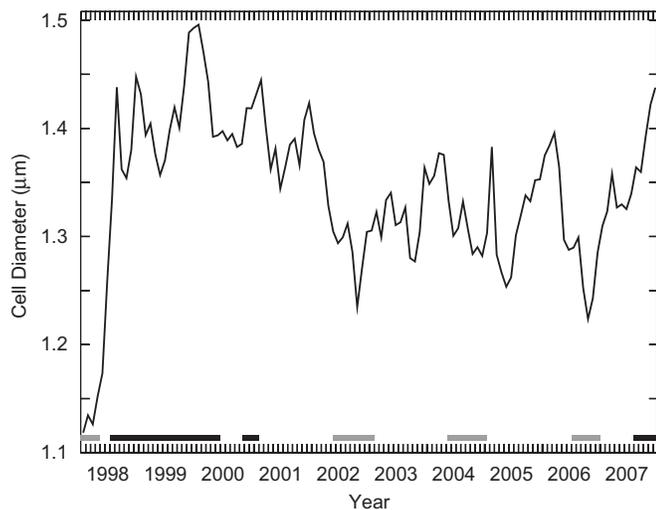

Fig. 2. Monthly mean cell diameter estimated using remotely sensed variables averaged over the Pacific equatorial upwelling region, 10°S–10°N, east of 180°. Gray and black lines above the date axis indicate El Niño and La Niña periods respectively.

Table 1
Results of the GAM. Initial phytoplankton cell diameter (M_{D50}) and percent change over the period 1998–2007 are estimated from the linear trend lines (Figs. 3 and 4). The adjusted R^2 is for the fit of GAM while the p-value is for the slope of the linear trend (Figs. 3 and 4) ($N=120$ for each region).

Subtropical region	GAM adj. R^2	Initial M_{D50} (μm)	% Change in M_{D50} over 1998–2007	p-Value
North Pacific	0.95	1.05	−2.2	< 0.0001
South Pacific	0.95	1.09	−2.3	< 0.0001
North Atlantic	0.92	1.22	−4.3	< 0.0001
Northern Hemisphere	0.97	1.10	−2.8	< 0.0001
Southern Hemisphere	0.98	1.14	−1.4	0.01
Global	0.84	1.12	−2.1	< 0.0001

southern hemisphere M_{D50} diameters of 2.8% and 1.4%, respectively, over the period 1998–2007 (Table 1, Fig. 4). Lastly, combining the data globally, the linear trend in the GAM estimated statistically significant declines in median cell diameter of 2.1% (Table 1, Fig. 4).

The frequency distributions of the median phytoplankton diameters grouped by size categories and pooled over 3 years at the beginning and end of the time series show that the 0.75–1.25 μm size grouping is the dominant size category in Pacific and North Atlantic subtropical oceans and the median phytoplankton size distribution is shifted slightly to larger phytoplankton in the North Atlantic compared to the other two regions (Fig. 5). Comparisons of the median size frequency between the beginning and end of the time series within regions show shifts toward smaller diameters in all three subtropical oceans over time (Fig. 5). In the North Pacific and North Atlantic, the frequency distributions at the end of the time series show an increase in phytoplankton in the 0.75–1.25 μm size range and a decrease in the 1.25–1.75 μm size range relative to the frequency distributions at the beginning of the time series (Fig. 5). In the South Pacific it was the smallest size category (< 0.75 μm) that had an increase in phytoplankton with the decrease occurring in the 0.75–1.25 μm size range (Fig. 5).

4. Discussion

The spatial distribution of median phytoplankton size estimated over the North Pacific for one winter and one summer month is consistent with our current understanding of the global phytoplankton size distribution and consistent with functional group types estimated from SeaWiFS chlorophyll (Kostadinov et al., 2010; Hirata et al., 2011). The subtropics contain a high proportion of picoplankton, nanoplankton are dominant in the subarctic and equatorial upwelling regions, while microplankton are most abundant in high latitude coastal regions (Hirata et al., 2011).

The decline (increase) in phytoplankton size during El Niños (La Niñas) in the equatorial upwelling region observed from our time series of phytoplankton median size is consistent with the nutrient dynamics with lower (higher) nutrients during El Niños (La Niñas) resulting primarily in a decrease (increase) in larger phytoplankton (Bidigare and Ondrusek, 1996; Landry et al., 1997; DiTullio et al., 1993). For example, during a moderate El Niño, the proportion of phytoplankton smaller than 2 μm was observed to be about 10% higher as a percent of total chlorophyll and the proportion of phytoplankton greater than 14 μm was 75% lower compared to a non-El Niño period at the equator and 140°W longitude (Bidigare and Ondrusek, 1996). Further, an examination
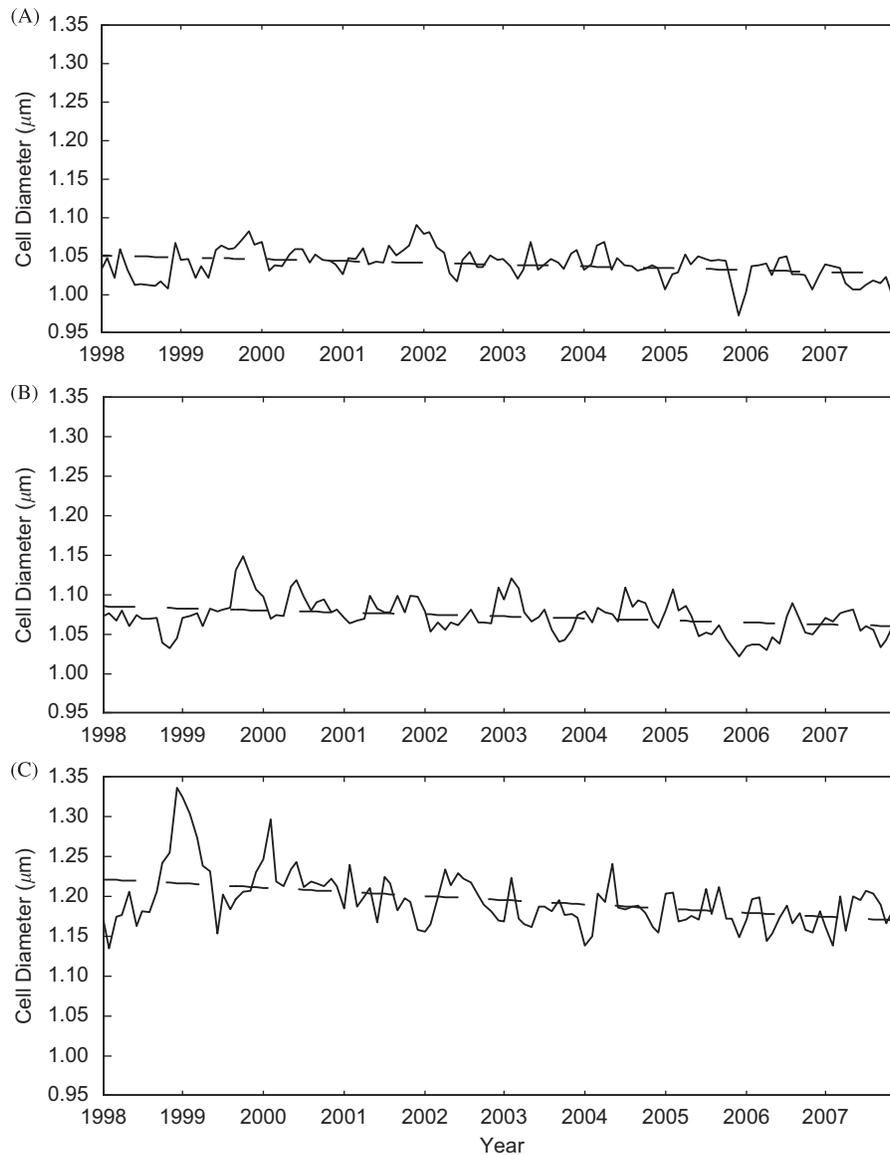
Fig. 3). The North Atlantic subtropical ocean had an initial M_{D50} diameter of 1.22 μm which declined by 4.3% over the period 1998–2007 (Table 1, Fig. 3). Pooling the cell size data from all subtropical oceans, including the South Atlantic and South Indian Oceans, for each hemisphere, the linear trend in the GAM estimated statistically significant declines in northern and

Fig. 3. Time series and linear trend of cell diameter estimated using remotely sensed variables with seasonal component removed between 10 and 30°N latitude in North Pacific (A), South Pacific (B), and North Atlantic (C), 1998–2007.

of the change in satellite remotely-sensed phytoplankton production by functional groups during the 1998–1999 El Niño and La Niña event in the Pacific equatorial upwelling region also found a strong shift in primary production from microplankton and nanoplankton (Uitz et al., 2010). Microplankton, nanoplankton, and picoplankton production anomalies decreased by 37%, 21%, and 8% respectively in response to the 1998 El Niño and increased by 53%, 13%, and 3% in response to the 1999 La Niña (Uitz et al., 2010).

The estimated 38% increase in median phytoplankton cell diameter estimated between the 1998 El Niño and the subsequent La Niña suggests that the equatorial upwelling pelagic food chain may routinely experience interannual variation in size that will impact energy transfer to higher levels. The estimated 2–4% decline in median phytoplankton diameter in three subtropical oceans over the period 1998–2007 suggests that food web length may vary on decadal and basin-scales as well. The decline in median phytoplankton size in the three subtropical oceans is consistent with the 1–4%/year areal expansion of the most oligotrophic core of the subtropical gyres, the region with the

highest proportion of picoplankton, in the North and South Pacific and Atlantic estimated from SeaWiFS data, 1998–2006 (Polovina et al., 2008). The decade-long phytoplankton size time series likely incorporates influences from interannual, decadal, and global warming forcing. For example, decadal forcing, specifically the Pacific Decadal Oscillation (PDO) and the Atlantic Multi-decadal Oscillation (AMO), have been shown to be an important factor in the dynamics of 20-year global satellite remotely-sensed chlorophyll and SST time series (Martinez et al., 2009). The PDO and AMO have not changed phase since 1999 so they may not be a significant factor in our shorter time series. ENSO, on the other hand, could be a factor for our time series since it begins in 1998 with strong El Nino and La Nina events followed by several weak and moderate El Ninos before ending with the beginnings of a moderate La Nina in 2007. Lastly, the estimated decline in median phytoplankton size is also consistent with the likely response from global warming. Specifically, an increase in small phytoplankton has been proposed as a universal response to warmer temperatures (Moran et al., 2010; Daufresne et al., 2009). Further, an increase in ocean acidification has been linked to declines in
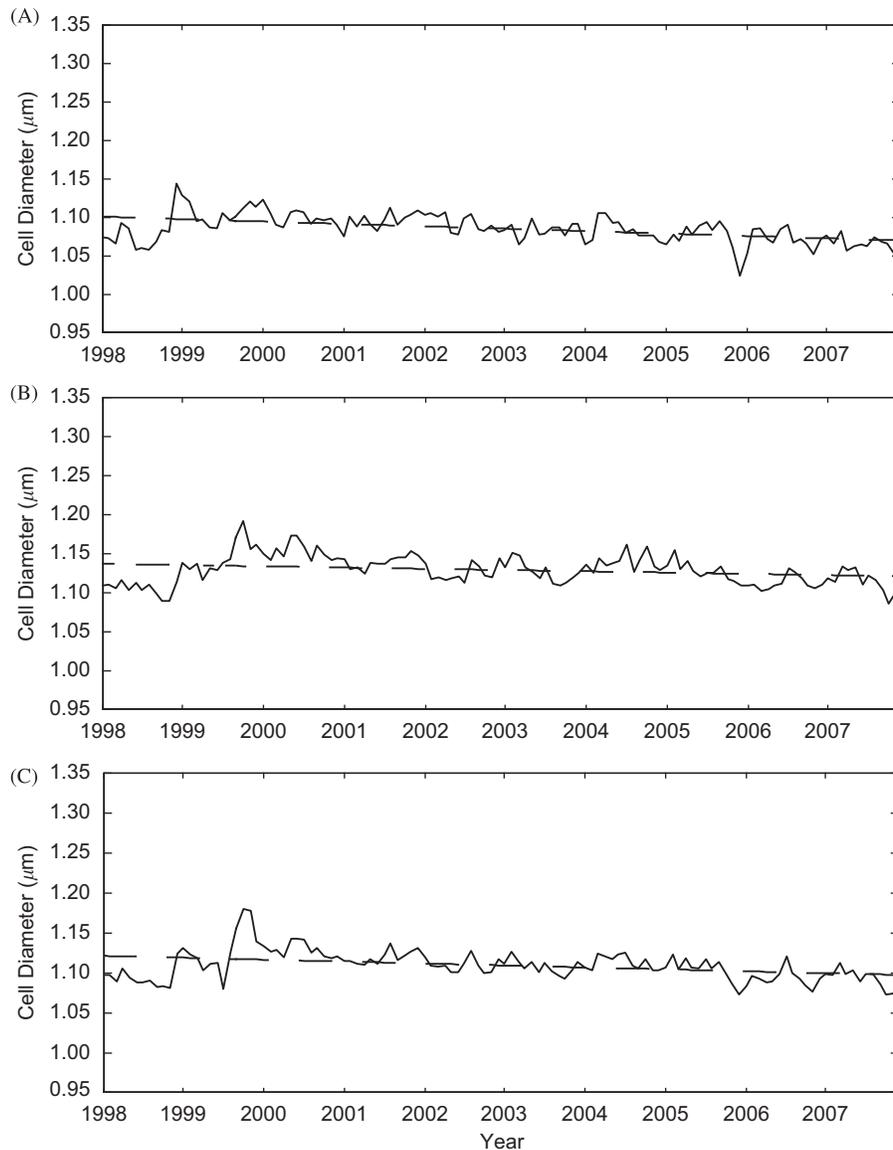
Fig. 4. Time series and linear trend of estimated cell diameter with seasonal component removed between 10 and 30°N latitude in the Northern Hemisphere (A), Southern Hemisphere (B), and global ocean (C), 1998–2007.

oceanic nitrification rates which could also result in a shift to smaller sized phytoplankton (Beman et al., 2011). The output from a global climate model that includes a coupled phytoplankton model estimated a 7% decline in the percent of large phytoplankton in the North Pacific subtropical biome over the 21st century (Polovina et al., 2011). However, this model result represents the mean over a dynamic subtropical biome which expands by 30% over the century and may underestimate the decline in a subtropical region of fixed dimension that we used. Our mean phytoplankton time series is too short to attribute the decline in median phytoplankton solely to global warming but this model approach can serve as an important method to monitor future ecosystem impacts from climate change and provide feedback to climate ecosystem models.

The frequency distributions of median phytoplankton sizes estimated for the Pacific and North Atlantic subtropical oceans are consistent with field studies from the oligotrophic Atlantic which estimated that picoplankton (< 2 μm) accounted for 80–90% of the total chlorophyll (Jochem and Zeitzschel, 1993; Maranon et al., 2001). The frequency distributions also provide insights on the relative phytoplankton size structure between the three

subtropical regions and changes over time within regions. In all three subtropical oceans the decline in median phytoplankton size was a result of the shift of the median size frequency distribution to smaller sized phytoplankton.

Estimation of median phytoplankton size from two remotely-sensed variables appears to provide useful global and potentially long term time series to aid in our understanding of pelagic ecosystem dynamics in response to climate change. A key to maintaining a long term median phytoplankton time series is the availability of long term satellite remotely-sensed SST and chlorophyll time series. Remotely-sensed SST is the variable that has received the most attention from a product development and operational perspective, with an SST time series going back to 1985. It is likely future satellite missions will overlap and estimates will be inter-calibrated so long time series of comparable SST measurements will be maintained. Maintaining a similar long time series of comparable chlorophyll estimates is more uncertain. SeaWiFS data has ended and extending it with MODIS data is difficult as the estimates of surface chlorophyll from the two sensors for the same location and time often do not exactly match. There is a blended chlorophyll product, called Globcolour
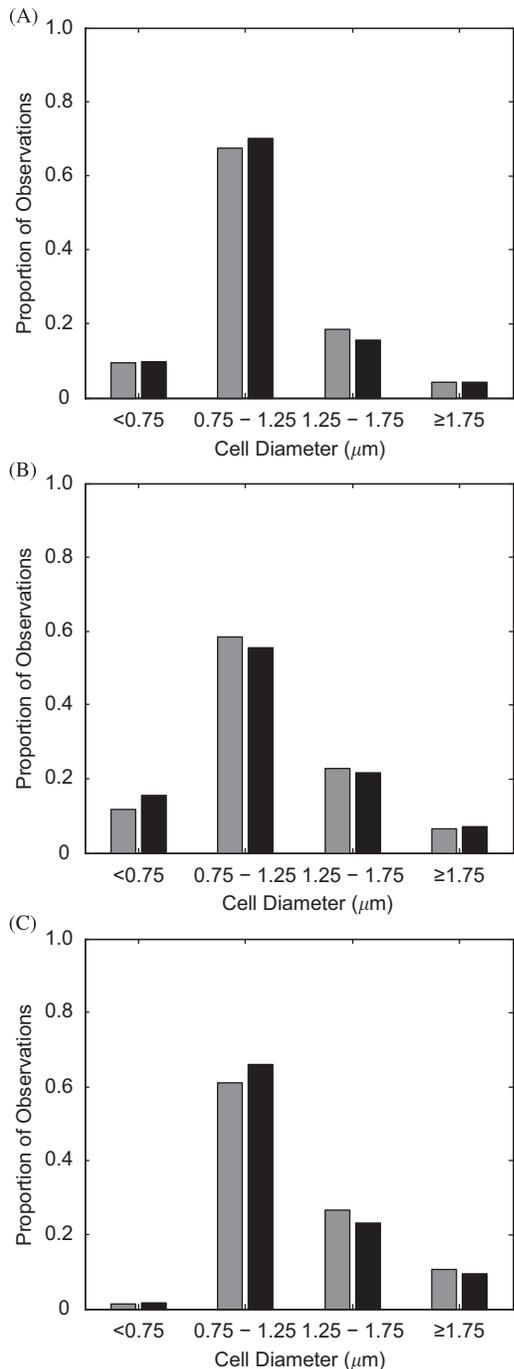
remotely-sensed SST and chlorophyll are available weekly and even on finer time steps but data loss due to cloud cover increases substantially as temporal resolution is increased. Thus, temporal resolution that is finer than monthly is not practical for most locations. Another caveat is the empirical model we use to estimate median size was derived from changes across ecosystems, yet we are using it to estimate changes over time within a region. This assumes that the relationship between phytoplankton size and chlorophyll and SST are the same within an ecosystem as between ecosystems. Another possible limitation of the empirical model is that we assume the relationship between median size and chlorophyll and SST does not change over time if the phytoplankton community changes. Maintaining a time series of field measurements of phytoplankton size structure over a range of ocean habitats and conducting statistical analysis both within and between habitats is critical to understanding and updating this and other satellite remotely-sensed methodologies.

5. Conclusions

We show that satellite remotely-sensed data can be used, especially in the subtropical and equatorial regions, to estimate a time series of median phytoplankton size. The results suggest that phytoplankton median cell size can vary substantially in the Pacific equatorial upwelling region in response to ENSO events and has declined 2–4% over the past decade in 3 subtropical oceans. This empirical model provides an approach to monitor an aspect of phytoplankton size structure that exhibits temporal dynamics over biome-scales and may represent an important ecosystem indicator of climate change.

Fig. 5. Frequency distribution of median cell diameter estimated using remotely sensed variables for the subtropical regions of the North Pacific (A), South Pacific (B), and North Atlantic (C) for 1998–2000 (gray) and 2005–2007 (black).

(www.globcolour.org), produced by the European Space Agency providing a chlorophyll time series from 1998 to the present derived from blending estimates from SeaWiFS, MODIS, and Medium Resolution Imaging Spectrometer (MERIS) which may address the need for long-term chlorophyll time series.

There are limitations to the use of an empirically-derived equation to estimate median phytoplankton size from two remotely-sensed variables. Loss of data from cloud cover in higher latitudes makes it difficult to generate monthly time series for all regions of the globe. The spatial resolution for each data point is 11 km^2 which is extremely coarse compared to in-situ sampling. We used monthly temporal resolution although both satellite

References

Alvain, S., Moulin, C., Dandonneau, Y., Breon, F.M, 2005. Remote sensing of phytoplankton groups in case 1 waters from global SeaWiFS imagery. Deep-Sea Res. I 52 (11), 1989–2004.

Agawin, N.S.R., Duarte, C.M., Agusti, S., 2000. Nutrient and temperature control of the contribution of picoplankton to phytoplankton biomass and production. Limnol. Oceanogr. 45 (3), 591–600.

Barnes, C., Irigoien, X., De Oliveira, J.A.A., Maxwell, D., Jennings, S., 2011. Predicting marine phytoplankton community size structure from empirical relationships with remotely sensed variables. J. Plankton Res. 33 (1), 13–24.

Beman, J.M., Chow, C., King, A.L., Feng, Y., Fuhrman, J.A., Andersson, A., Bates, N.R., Popp, B.N., Hutchins, D.A., 2011. Global declines in oceanic nitrification rates as a consequence of ocean acidification. PNAS 108 (1), 208–213.

Bidigare, R.R., Ondrusek, M.E., 1996. Spatial and temporal variability of phytoplankton pigment distribution in the central equatorial Pacific Ocean. Deep-Sea Res. II 43, 809–833.

Blanchard, J.L., Jennings, S., Law, R., Castle, M.D., McCloghrie, P., Rochet, M., Benoit, E., 2009. How does abundance scale with body size in couple size-structured food webs? J. Anim. Ecol. 78, 270–280.

Brewin, R.J.W., Hardman-Mountford, N.J., Lavender, S.J., Raitsos, D.E., Hirata, T., Uitz, J., Devred, E., Bricaud, A., Ciotti, A., Gentili, B., 2011. An intercomparison

of bio-optical techniques for detecting dominant phytoplankton size class from satellite remote sensing. Remote Sensing Environ. 115, 325–339.

Daufresne, M., Lengfellner, K., Sommer, U., 2009. Global warming benefits the small in aquatic ecosystems. PNAS 31 (106), 12788–12793.

DiTullio, G.R., Hutchins, D.A., Bruland, K.W., 1993. Interaction of iron and major nutrients controls phytoplankton growth and species composition in the tropical North Pacific. Limnol. Oceanogr. 38 (3), 495–508.

Hirata, T., Hardman-Mounford, N.J., Brewin, R.J., Aiken, J., Barlow, R., Suzuki, K., Isada, T., Howell, E., Hashioka, T., Noguchi-Aita, M., Ymanaka, Y., 2011. Synoptic relationships between surface chlorophyll-a and diagnostic pigments specific to phytoplankton functional types. Biogeosciences 8, 311–327.

Jochem, F.J., Zeitzschel, B., 1993. Productivity regime and phytoplankton size structure in the tropical and subtropical North Atlantic spring 1989. Deep Sea Res. II 40, 495–519.

Kostadinov, T.S., Siegel, D.A., Maritorena, S., 2010. Global variability of phyto-plankton functional types from space: assessment via the particle size distribution. Biogeosciences 7, 3239–3257.

Landry, M.R., Barber, T.R., Bidigare, R.B., Chai, F., Coale, K.H., Dam, H.G., Lewis, M.R., Lindley, S.T., McCarthy, J.J., Roman, M.R., Stoecker, D.K., Verity, P.G., White, J.R., 1997. Iron and grazing constraints on primary production in the central equatorial Pacific: an EqPac synthesis. Limnol. Oceanogr. 42 (3), 405–418.

Maranon, E., Hollogan, P.M., Barciela, R., Gonzalez, N., Mourino, B., Pazo, M.J., Varela, M., 2001. Patterns of phytoplankton size structure and productivity in contrasting open-ocean environments. Mar. Ecol. Prog. Ser. 216, 43–56.

Martinez, E., Antoine, D., D'Ortenzio, F., Gentili, B., 2009. Climate-driven basin-scale decadal oscillations of oceanic phytoplankton. Science 326, 1253–1256.

Menden-Deuer, S., Lessard, E.J., 2000. Carbon to volume relationships for dino-flagellates, diatoms, and other protest plankton. Limnol. Oceanogr. 45, 569–579.

Moran, X.A., Lopez-Urrutia, A., Calvo-Diaz, A., Li, W.K.W., 2010. Increasing importance of small phytoplanlton in a warmer ocean. Global Change Biol. 16, 1137–1144.

Polovina, J.J., Howell, E.A, Abecassis, M., 2008. The ocean's least productive waters are expanding. Geophys. Res. Lett. 35, L03618, http://dx.doi.org/10.1029/2007GL031745.

Polovina, J.J., Dunne, J.P., Woodworth, P.A., Howell, E.A., 2011. Projected expansion of the subtropical biome and contraction of the temperate and equatorial upwelling biomes in the North Pacific under global warming. ICES J. Mar. Sci. 68 (6), 986–995.

Sprules, W.G., Munawar, M., 1986. Plankton size spectra in relationship to ecosystem productivity, size and perturbation. Can. J. Fish. Aquat. Sci. 43, 1789–1794.

Uitz, J., Claustre, H., Gentili, B., Stramski, D., 2010. Phytoplankton class-specific primary production in the world's oceans: seasonal and interannual variability from satellite observations. Global Biogeochem. Cycles 24, 1–19, http://dx.doi.org/10.1029/2009GB003680.

Yoder, J.A., Doney, S.C., Siegel, D.A., Wilson, C., 2010. Study of marine ecosystems and biogeochemistry now and in the future. Oceanography 23 (4), 104–117.